ORGANIC LETTERS

2006
Vol. 8, No. 21
4691−4694

Phenylalanine 445 within Oxidosqualene–Lanosterol Cyclase from *Saccharomyces cerevisiae* Influences C-Ring Cyclization and Deprotonation Reactions

Tung-Kung Wu,* Yuan-Ting Liu, Feng-Hsuan Chiu, and Cheng-Hsiang Chang

Department of Biological Science and Technology, National Chiao Tung University, 300, Hsin-Chu, Taiwan, Republic of China

tkwmll@mail.nctu.edu.tw

Received June 23, 2006

ABSTRACT

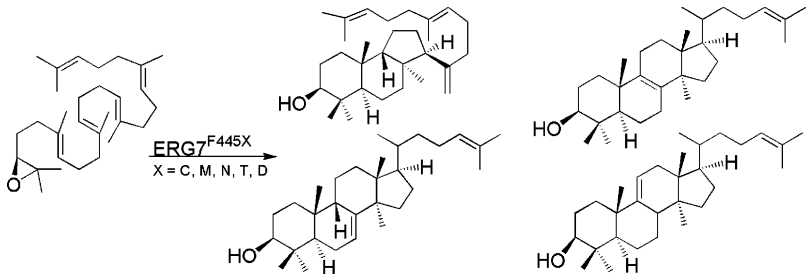

We describe the *Saccharomyces cerevisiae* oxidosqualene–lanosterol cyclase Phe445 site-saturated mutants that generate truncated tricyclic and altered deprotonation product profiles. Among these mutants, only polar side-chain group substitutions genetically complemented yeast viability and produced spatially related product diversity, supporting the Johnson model that cation–π interactions between a carbocationic intermediate and an enzyme can be replaced by an electrostatic or polar side chain to stabilize the cationic intermediate, but with product differentiation.

Oxidosqualene cyclases catalyze the cationic cyclization/rearrangement of (3*S*)-2,3-oxidosqualene (OS) into a variety of sterols and triterpenes.[1] The postulated cationic mechanism of the cyclization/rearrangement cascade is initiated by epoxide protonation, followed by tetracyclic ring annulation and a series of rearrangements of hydride and methyl groups, and culminates with a highly specific deprotonation step. The diverse product profile is mainly generated through the alteration of the precise regulation that exists between the substrate and the enzyme, as well as through the changes of interactions between crucial functional groups of the active site residues and the cationic intermediates for deprotonation.

Recently, we and others applied genetic selection, which was coupled with a product isolation strategy, to identify the critical amino acid residues that are involved in determining the cyclization/rearrangement outcome, or the changing of product specificity from cycloartenol production to lanosterol formation.[2,3] In parallel, X-ray crystallographic analysis of two cyclases, bacterial squalene−hopene cyclase (SHC) and human oxidosqualene−lanosterol cyclase (OSC),

(1) (a) Abe, I.; Rohmer, M.; Prestwich, G. D. *Chem. Rev.* **1993**, *93*, 2189−2206. (b) Wendt, K. U.; Schulz, G. E.; Corey, E. J.; Liu, D. R. *Angew. Chem., Int. Ed.* **2000**, *39*, 2812−2833. (c) Xu, R.; Fazio, G. C.; Matsuda, S. P. T. *Phytochemistry* **2004**, *65*, 261−291. (d) Wendt, K. U. *Angew. Chem., Int. Ed.* **2005**, *44*, 3966−3971.

(2) (a) Wu, T. K.; Griffin, J. H. *Biochemistry* **2002**, *41*, 8238−8244. (b) Wu, T. K.; Chang, C. H. *ChemBioChem* **2004**, *5*, 1712−1715. (c) Wu, T. K.; Liu, Y. T.; Chang, C. H. *ChemBioChem* **2005**, *6*, 1177−1181. (d) Wu, T. K.; Yu, M. T.; Liu, Y. T.; Chang, C. H.; Wang, H. J.; Diau, E. W. G. *Org. Lett.* **2006**, *8*, 1319−1322. (e) Wu, T. K.; Liu, Y. T.; Chang, C. H.; Yu, M. T.; Wang, H. J. *J. Am. Chem. Soc.* **2006**, *128*, 6414−6419.

10.1021/ol061549r CCC: $33.50
Published on Web 09/21/2006

has greatly facilitated the interpretation of the catalytic cyclization/rearrangement reaction mechanism, as well as the diverse profile and functional role of the specific residue.[4] However, the relationships between protein evolution and product specificity remain unclear.

We previously identified five single-point mutations of the *Arabidopsis thaliana* oxidosqualene−cycloartenol synthase (CAS), which were found to possess altered cyclase activity compared with that of *Saccharomyces cerevisiae* oxidosqualene−lanosterol cyclase (ERG7).[2a] A detailed analysis of the mutated sequences revealed that three out of five random mutations (i.e., Ala469, His477, Ile481) occurred within a region that was 15 residues upstream of the putative active site, Asp-483, of the CAS enzyme. The clustering of these product-altering mutations in this region indicated its importance in protein evolution and led to the speculation that this region might also be conserved in many cyclases for the crucial determination of the cyclization/rearrangement cascade or cyclase product diversity. In addition, crystallographic analysis of human OSC revealed that a conserved side chain of Phe444 (which corresponds to Phe445 and 11 residues upstream of the putative active site Asp456 of *S. cerevisiae* ERG7) was observed to stabilize the intermediate tertiary cations at both C6 and C10 after both A- and B-ring formation through cation-π interactions.[4c] Therefore, a series of amino acid residues, sequences ^{441}GAWGFSTKTQGYT^{453} within this region of *S. cerevisiae* ERG7, were subjected to both alanine-scanning mutagenesis and plasmid shuffle selection for the identification of possible residues involved in the complementation of cyclase-deficient yeast strains.

Several inactive mutations were identified, including the Phe445Ala mutation, that failed to complement the cyclase deficiency. To further determine the functional role of Phe445 and to investigate the effects of substitutions of this residue on other proteinogenic amino acids in terms of catalysis and product specificity, we genetically selected Phe445 site-saturated mutants (F445X) and characterized each mutant product. We report, within this context, the results of the F445X site-saturated mutations, as well as the product profile determinations of each mutant. An interesting product profile, which specifically affected truncated tricyclic cyclization and/or final deprotonation, was isolated from a strain that only expressed polar groups that substituted ERG7^{F445X} as their only oxidosqualene-cyclase. These results suggested a catalytic role for Phe445 in ERG7 catalysis that could affect cation stabilization at both the C14 position for tricyclic products and position C8/C9 for final deprotonation products.

The ERG7^{F445X} site-saturated mutations were generated using the QuickChange site-directed mutagenesis kit.[2d,e] The recombinant plasmids were then transformed into a yeast HEM1 ERG7 double-knockout mutant, TKW14, which is only viable when either supplied with exogenous ergosterol or when complemented with oxidosqualene cyclase activity derived from ERG7^{F445X}.[2a,b,5] The genetic selection results showed that the F445X mutations resulted in nonviable TKW14[pERG7^{F445X}] mutants, except for the Cys, Met, Asn, Thr, and Asp substitutions. These results indicated that this position is crucial for the catalytic function of the enzyme.

We next cultured the TKW14[pERG7^{F445X}] mutant strains and isolated the nonsaponifiable lipid (NSL) extracts for product characterization. Gas chromatography−mass spectrometry (GC−MS) was used to assay the triterpenoid products with a molecular mass of $m/z = 426$. No products with $m/z = 426$ were observed for the above-mentioned nonviable mutants, consistent with the genetic selection results. For the viable mutants, four identical products with different product ratios were identified (Table 1). Identical retention times and mass spectral characteristics on GC−MS, as well as spectroscopic profiles on NMR, confirmed the structures of the compounds as (13α*H*)-isomalabarica-14(26),17*E*,21-trien-3β-ol, 9β-lanosta-7,24-dien-3β-ol ($\triangle^7$-lanosterol), lanosterol, and parkeol, compared with those published in the literature.[2c,e,3d,6] Interestingly, all viable mutants affected the formation of products either proximal to the B/C ring junction or upon C-ring formation, which affected the deprotonation and cyclization steps, respectively. No monocyclic, bicyclic, tetracyclic, or truncated rearrangement products were observed in the GC−MS analyses from any of the mutants.

Table 1. Product Profiles of *S. cerevisiae* TKW14 Expressing the ERG7^{F445X} Site-Saturated Mutants[7, a]

amino acid substitution	(13αH)-iso-malabarica-14(26)-17*E*,21-trien-3β-ol	lanosterol	parkeol	9β-lanosta-7,24-dien-3β-ol
native		100	0	
F445C	10	69	13	8
F445M	7	65	18	10
F445N	10	63	9	18
F445T	49	46	0	5
F445D	21	63	11	5

[a] Neither cell viability nor product was characterized for the rest of the ERG7^{F445X} mutants.

In the ERG7^{F445X} viable mutants, oxidosqualene is folded in a chair−boat−chair conformation and undergoes cationic cyclization to a tricyclic C14 cation without disruption at either the monocyclic or bicyclic cationic positions. This is followed by direct deprotonation from Me-26 to generate (13α*H*)-isomalabarica-14(26),17*E*,21-trien-3β-ol. Further-

(3) (a) Hart, E. A.; Hua, L.; Darr, L. B.; Wilson, W. K.; Pang, J.; Matsuda, S. P. T. *J. Am. Chem. Soc.* **1999**, *121*, 9887−9888. (b) Joubert, B. M.; Hua, L.; Matsuda, S. P. T. *Org. Lett.* **2000**, *2*, 339−341. (c) Matsuda, S. P. T.; Darr, L. B.; Hart, E. A.; Herrera, J. B. R.; McCann, K. E.; Meyer, M. M.; Pang, J.; Schepmann, H. G.; Wilson, W. K. *Org. Lett.* **2000**, *2*, 2261−2263. (d) Herrera, J. B. R.; Wilson, W. K.; Matsuda, S. P. T. *J. Am. Chem. Soc.* **2000**, *122*, 6765−6766. (e) Meyer, M. M.; Xu, R.; Matsuda, S. P. T. *Org. Lett.* **2002**, *4*, 1395−1398. (f) Lodeiro, S.; Schulz-Gasch, T.; Matsuda, S. P. T. *J. Am. Chem. Soc.* **2005**, *127*, 14132−14133. (g) Lodeiro, S.; Wilson, W. K.; Shan, H.; Matsuda, S. P. T. *Org. Lett.* **2006**, *8*, 439−442.

(4) (a) Wendt, K. U.; Poralla, K.; Schulz, G. E. *Science* **1997**, *277*, 1811−1815. (b) Wendt, K. U.; Lenhart, A.; Schulz, G. E. *J. Mol. Biol.* **1999**, *286*, 175−187. (c) Thoma, R.; Schulz-Gasch, T.; D'Arcy, B.; Benz, J.; Dehmlow, H.; Hennig, M.; Stihle, M.; Ruf, A. *Nature (London)* **2004**, *432*, 118−122.

(5) Shi, Z.; Buntel, C. J.; Griffin, J. H. *Proc. Natl. Acad. Sci. U.S.A.* **1994**, *91*, 7370−7374.

(6) Segura, M. J. R.; Lodeiro, S.; Meyer, M. M.; Patel, A. J.; Matsuda, S. P. T. *Org. Lett.* **2002**, *4*, 4459−4462.

more, C-ring expansion was followed by D-ring annulation to generate the protosteryl C20 cation. A series of skeletal rearrangements, including hydride and methyl group shifts, then generates the lanosteryl C8/C9 cation. 9β-Lanosta-7,-24-dien-3β-ol is conceivably derived by the stabilization of the C8 cation, which undergoes deprotonation at the C7 position. Lanosterol is formed by a final deprotonation step, either abstracting the proton originally at C9 or after a hydride shift from C9 to C8. Parkeol is preferentially rationalized by stabilizing the C9 cation via a hydride shift from H-9β to H-8β, which undergoes deprotonation at the C11 position.

The effects of amino acid mutations on enzymatic activity, the formation of derailment products, and relative product proportions are complicated and are only partially understood. We applied homology modeling of the *S. cerevisiae* ERG7, which was derived from the human OSC X-ray crystal structure, to investigate how the polar side-chain substitution of Phe445 results in truncated tricyclic and altered deprotonation products (Scheme 1). Alignment of

Scheme 1. Product Profile Produced by *S. cerevisiae* TKW14 Expressing the ERG7^{F445X} Site-Saturated Mutations

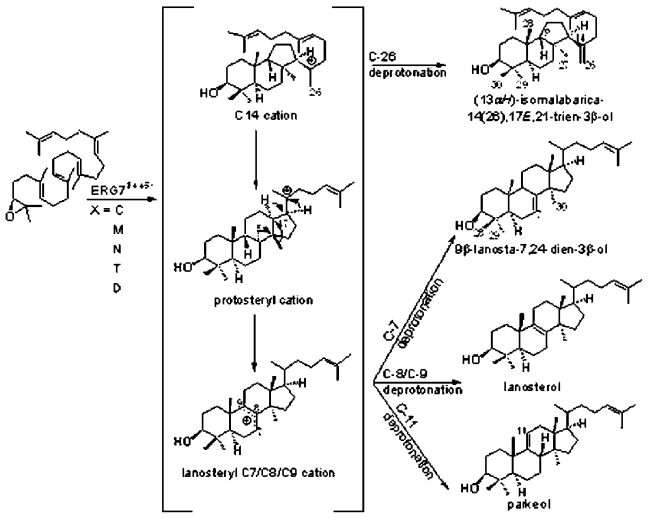

multiple sequences revealed that Phe445 of ERG7 is conserved among all known triterpene cyclase enzymes, except for β-amyrin synthase from *Avena strigosa*, and was aligned with Phe365 of SHC and Phe444 of human OSC, respectively. Based on the X-ray structure of both the bacterial SHC and human OSC sequences, both Phe365 and Phe444 were suggested to be involved in the stabilization of the third cation of the cyclization cascade at atom C8.[4b,c] Moreover, the substitution of alanine for Phe365 caused a destabilization of the cation$-\pi$ interaction between the C8 carbocation of hopene and the aromatic side chain of Phe, and thus, quenched the cyclization reactions at the bicyclic stage during the squalene$-$hopene cyclization cascade.[4a,b,8] Homology modeling of the *S. cerevisiae* ERG7 also revealed that Phe445 of ERG7 is also spatially proximal to both the B/C ring fusion and to the C8 and C14 positions, which are occupied directly above the cationic center during protosteryl cation formation. The observed π-electrons of Phe445 were found at a distance of approximately 5.1 and 5.8 Å to the C8 and the C14 of lanosteryl cation, respectively, which agree with the cation-π interactions for the observed aromatic amino acid residues in the lanosterol C8 cation-bound OSC complex (Figure 1).

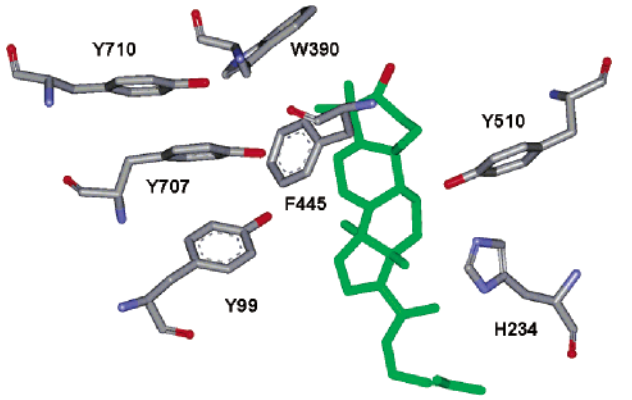

Figure 1. ERG7 residues form a putative π-electron pocket and interact with the lanosteryl C8 cation in the homology model structure.

The careful examination of the mutants' homology models suggested that the electronic differences between the Phe445 and polar side-chain groups of similarly sized amino acid residues could account for the catalytic differences for the formation of lanosterol, parkeol, and 9β-lanosta-7,24-dien-3β-ol. Greater π-electron density near the C8/C9 positions of lanosterol with seven aromatic residues was suggested to be responsible for the equilibrium shift toward the C8/C9 cation and, subsequently, for the formation of lanosterol.[4c] The terminal phenyl group of Phe445 was found to interact with Tyr99 (3.7 Å), Trp390 (4.4 Å), Tyr510 (6.5 Å), Tyr707 (4.0 Å), and Tyr710 (6.2 Å) (Figure 1). The π-electron-rich pocket created by these residues is optimal for the stabilization of the electron-deficient cationic intermediates. Substitutions of the Phe445 with Cys, Met, Asp, Asn, and Thr complemented cyclase-deficiency but resulted in the isolation of truncated tricyclic and alterted deprotonation products. Perhaps the transient cation$-\pi$ interaction, between the carbocationic intermediate and the enzyme, could be replaced by an electrostatic or polar amino acid of similar size to stabilize the cationic intermediate, previously proposed by Johnson's model.[9] However, the changes caused by these modified electrostatic or polar interactions may slightly retard the folding of the D-ring, which would then allow some deprotonation or directly abstract the C26 proton to form

(7) The in vivo TKW14[pERG7^{F445X}] product profiles represent metabolic equilibrium of lanosterol and related triterpenes under physiological conditions, which may vary from that of in vitro assay.

(8) (a) Hoshino, T.; Sato, T. *Chem. Commun.* **1999**, 2005$-$2006. (b) Reinert, D. J.; Balliano, G.; Schulz, G. E. *Chem. Biol.* **2004**, *11*, 121$-$126.

(9) Johnson, W. S. *Tetrahedron* **1991**, *47*, xi-1.

the truncated tricyclic (13α*H*)-isomalabarica-14(26),17*E*,21-trien-3β-ol product. In contrast, the mutation of Phe445 to a nonpolar hydrophobic side chain, such as Gly, Ala, Val, Leu, and Ile, may disrupt either the cation-π or electrostatic interactions in the active site cavity compared with those of the wild-type enzyme.

The steric or orientation of the side chains also exhibited a significant effect on the enzyme's catalytic activity. The mutation of Phe445 to Trp reduced the size of the cavity of the active site. This, in turn, obstructed cyclase structural integrity for either substrate binding or intermediate stabilization, and resulted in the abolishment of lanosterol biosynthesis, consistent with the experimental data. Similarly, the increased steric from Asp to Glu, as well as from Asn to Gln, also abolished cyclase activity. The ERG7^{F445Q} mutant abolished cyclase activity by shifting the cavity of the active site and disrupting the π-electron-rich pocket (data not shown). Computer models have showed that the mutation of Phe445 to a side chain such as Ser enlarges the cavity of the active site and subsequently disrupts the transient dipole interactions between the Ser hydroxyl group and the carbocationic intermediate.[8b] This minor reduction of the ligand-enzyme interaction resulted in the formation of the inactive mutant.

We note that the polar side chain subtitutions at the Phe445 position of ERG7 specificically generated truncated tricyclic and altered deprotonation product profiles proximal to both the B/C ring junction and the C8 and C14 positions. These mutations caused multiple abortive and/or alternative cyclization/rearrangement products, ranging from monocyclic, tricyclic, tetracyclic, and truncated rearrangments to altered deprotonation from the site-saturated mutagenesis of ERG7^{H234X} mutants.[2e] The homology modeling of ERG7 showed that Phe445 and His234 are located in different parts of the active site cavity, with a relative distance of 5.1 and 5.0 Å, respectively, to the C8 cation; the latter hydrogen bonds interact with Tyr510. The substitution of His234 by various amino acid side chains introduced either steric or electrostatic effects on the intrinsic His234:Tyr510 H-bonding network, subsequently altering the spatial location or cation-π interaction between the intermediate carbocation and phenolic oxygen of Tyr510. The distance between the phenyl group of Phe445 and Tyr510 corresponds to more than 6.5 Å. A mutation at the Phe445 position exhibited little or no direct effect on either His234 or Tyr510, although Tyr510 was involved in the π-electron-rich pocket of the active-site cavity. This may account for the product specificity of ERG7^{F445X} site-saturated mutations on the formation of truncated tricyclic and altered deprotonation products; the ERG7^{H234X} site-saturated mutations generated diverse product profiles, based on the steric effects that altered either the active-site cavity structure or the electrostatic effects on the His234:Tyr510 H-bonding network.

In summary, our genetic selection-product characterization strategy uncovered the catalytic function and product profile of the Phe445 residue in the ERG7-catalyzed cyclization/rearrangement cascade. The characterization of the truncated tricyclic product and the altered deprotonation products, which were spatially located near the C ring or B/C ring fusion, suggests the catalytic role of the residue in affecting the cationic stabilization at the C14 position for the tricyclic product and the C8/C9 position for final deprotonation product formation. In addition, the identification of the spatially related product profiles from different cyclase mutants supports the hypothesis that evolutionary divergence of the protein, in addition to product diversity, could be attained from subtle molecular interaction changes, which are derived from structural modification or electronic differentiation of active site residue substitution or reposition. Finally, our results exemplify the power of site-saturated mutagenesis in the elucidation of structure−function relationships where limited site-directed mutagenesis cannot be achieved.

Acknowledgment. We thank the National Science Council of the Republic of China and MOE ATU Program for financial support of this research under Contract No. NSC-94-2113-M-009-011. We are grateful to Dr. John H. Griffin and Prof. Tahsin J. Chow for their helpful advice.

Supporting Information Available: Experimental methods and NMR spectra. This material is available free of charge via the Internet at http://pubs.acs.org.

OL061549R